



Grant Agreement Number: 956004

H2020-MSCA-ITN-2020

BIOTRIB

Advanced Research Training for the Biotribology of Natural and Artificial Joints in the 21st Century

Deliverable Report

Deliverable D4.5: Development of methodologies to quantify the degradation processes of implant-derived debris in real-time and in situ.

Project coordinator name	Prof. Richard M. Hall
Project coordinator organisation name	University of Leeds
Work Project	WP4
Supervisors	Prof. Michael Bryant Prof. Richard M. Hall Dr. Gregory de Boer
Report prepared by	Edona Hyla

Dissemination Level of Report: Public

PU	Public	X
PP	Restricted to other program participants (including the Commission Services)	
RE	Restricted to a group specified by the consortium (including the Commission Services)	
CO	Confidential, only for members of the consortium (including the Commission Services)	

The BioTrib ETN project has received funding from the European Union’s Horizon 2020 research and innovation programme under grant agreement No. 956004.



Version	Date	Comment	Modifications made by
D4.5.1	2023-08-10	First draft	ESR 15- Edona Hyla
D4.5.1	2023-08-19	Reviewed – Comments have been added	Richard M. Hall
D4.5.2	2023-09-11	Second draft submitted	ESR 15- Edona Hyla
D4.5.2	2023-09-11	Reviewed – Comments have been added	Richard M. Hall
D4.5.3	2023-09-21	Third draft submitted	ESR 15- Edona Hyla
D.4.5.3	2023-09-22	Reviewed – Comments have been added	Micheal G. Bryant
D.4.5.4	2023-10-04	Fourth draft submitted	ESR 15- Edona Hyla
D.4.5.4	2023-10-09	Reviewed – Comments have been added	Micheal G. Bryant
D.4.5.5	2023-10-12	Fifth draft submitted	ESR 15- Edona Hyla
D4.5	2023-11-09	Submitted to Commission	Judith Schneider (UNIVLEEDS)

Table of Contents

Deliverable 4.5	4
Chapter 1	5
1.1 Introduction.....	5
1.2 Aims and Objectives	6
Chapter 2	7
2.1 Introduction.....	7
2.2 Materials and methodology	7
2.2.1 Materials	8
2.2.2 Methodology.....	10
2.2.3 Analysing equipment.....	12
2.3 Summary	14
Chapter 3	15
3.1 Introduction.....	15
3.2 Aims and Objectives	16
3.3 Methodology	17
3.3.1 Debris Isolation	18
3.3.4 Methodology for preparation of ICP-MS for metallic trace analysis	19
3.3.5 Static corrosion ex-situ	20
3.3.5 Equipment.....	20
3.4 Summary	22
Chapter 4	23
4.1 In situ degradation methods for nanoparticles	23
4.2 Aims and Objectives	23
4.3 Equipment and Methodology.....	24
4.3.1 Equipment.....	24
4.3.2 Methodology.....	24
4.4 Summary	25
Chapter 5	26
5.1 Discussion and Conclusion.....	26
5.1.1 Discussion.....	26
5.1.2 Conclusion	26
References.....	27

Deliverable 4.5

The rationale for undertaking this project is underscored by the persistent concern surrounding the biological repercussions associated with wear debris and metal ions generated by metallic biomaterials employed in hip replacements [1]. In order to achieve significant reductions in wear and enhance the longevity and performance of hip replacements, it is imperative to delve deeper into the fundamental wear processes of implant materials and their interaction to the biological environment. Despite developments, there exists a distinct lack of in-depth understanding of the intricate mechanisms responsible for the generation of wear debris and metal ions within these implants [2]. A comprehensive grasp of these processes is pivotal to not only address the concerns related to wear debris and metal ions but also to innovate and refine the design and materials used in hip replacements.

Our project therefore aims to advance our comprehension of implant degradation mechanisms by investigating tribocorrosion phenomena in CoCrMo implant materials at both the micro and macro scale and furthermore it will analyse the characteristics of wear debris and elucidate their interactions with biological cells. This aim will be achieved by addressing the following objectives:

- **Tribocorrosion testing of CoCrMo** – Development of a methodology to monitor implant material degradation and debris generation, encompassing tribocorrosive responses under varying loads and potentials spanning at both macro and micro scales.
- **Wear debris analysis** – Conduct a comprehensive analysis of wear debris generated from the first objective. Including precise measurements of particle size, thorough examination of chemical composition and morphology, and rigorous investigation of ion concentration resulting from corrosion. Employ ex-situ analyses to gain profound insights into the characteristics and evolution of debris.
- **In-Situ Debris Analysis** – To employ in-situ analyses for gaining profound insights into the characteristics and evolution of debris, enabling real-time monitoring and assessment of its properties and behaviour.

Chapter 1

1.1 Introduction

Total hip replacement (THR) is documented to alleviate pain, rehabilitate, and elevate the overall quality of life [3]. Encouragingly, a substantial proportion, approximately 58% of THRs exhibit impressive longevity, lasting for a remarkable 25 years or more [4]. Nevertheless, the risk of requiring revision surgery due to adverse reactions still remains an issue [5].

Biomedical alloys undergo degradation processes that are inherently complex due to the combined effects of mechanical wear and corrosion [6]. The consequences of tribocorrosion are paramount in the context of periprosthetic soft-tissue reactions and the overall success of orthopaedic implants. The excessive release of wear debris and ions, adversely affects periprosthetic soft-tissue reactions and causes revision rates that exceed acceptable thresholds [7]. According to European Union Medical Device Regulation (EU MDR), devices must be designed and produced to ensure high levels of safety for orthopaedic patients [8,9].

Before implants are approved for use in clinical applications, extended wear and corrosion testing of artificial joints is performed. To conduct these tests, specialized equipment such as hip joint simulators is employed, adhering to established standards outlined in documents like ASTM (F2025) and ISO (14242, 14243, 18192). These standards provide methodologies and guidelines in the testing process, helping researchers and manufacturers assess the durability, performance, and safety of artificial joints. However, it's important to note that these tests, while valuable, have limitations [10,11]. The simulations conducted according to these standards aim to replicate in vivo conditions but are still simplified representations. They do not fully capture the complexities of the actual physiological environment, which includes variations in loading, motion, and biological responses. Moreover, those standards focus on individual aspects like wear or corrosion. Whereas, these factors can interact, influencing each other's behaviour. Furthermore, no understanding of the fundamental mechanisms in play is highlighted. Thus, it becomes apparent that there is a pressing need for enhancements to mitigate these limitations.

Achieving a minimal release of ions and other reaction byproducts into the body is desirable, and one way to accomplish this goal is by optimizing the surface features, such as topography of those interfaces [12]. However, the tribological and electrochemical mechanisms that emerge at the surface, especially the link between the latest to material behaviour and microstructure changes, are poorly understood [13,14].

Wimmer et. al. from retrieve hip joints has shown that a tribolayer formed on the surface is the origin of wear particles and their detachment into surrounding tissue [15]. Fischer et. al. took this concept into consideration and studied different biomaterials as well as their microstructure changes to relate this further to wear formation. However, testing was done at the macroscale in dry conditions, neglecting lubrication and corrosion mechanisms [16]. The lack of consideration for lubrication and corrosion mechanisms in their research hampers its clinical applicability. To address

this limitation, research efforts should aim to incorporate these critical factors into their investigations.

In the study conducted by Gilbert et al., an examination of metallic materials within a tribocorrosion environment was carried out utilizing an idealized single asperity test [17]. However, a notable limitation within their investigation lies in the absence of a substantiated linkage between interfacial properties and the observed tribocorrosive effects. Understanding how interfacial characteristics influence tribocorrosion phenomena is essential for a comprehensive understanding of implant degradation. Addressing this limitation can lead to improved implant materials and designs that are better suited to withstand the complex in vivo conditions. These limitations collectively underscore the need for a more comprehensive understanding of the complex interplay between tribocorrosion mechanisms, interfacial processes, and their translation to debris/ion formation. Knowing how tribocorrosion processes affect implant materials over time allows for the development of more durable and reliable implants, reducing the need for frequent replacements or revisions. In addition, understanding the interactions between wear debris, ions, and biological systems is essential for ensuring patient safety. It helps in identifying potential risks associated with specific implant materials and designs. As such, further research in this domain is imperative to bridge these knowledge gaps and advance our understanding of implant degradation mechanisms.

1.2 Aims and Objectives

Our primary aim was to develop a robust and systematic methodology specifically tailored to investigate the intricate process of wear formation within a tribocorrosive environment at the microscale. This methodology will bridge the existing gaps by establishing a direct link between asperity contact interactions and the underlying microstructural changes that drive wear phenomena. By focusing on this intricate interplay at the micro- macro- scale, we aim to unravel the underlying mechanisms that govern wear formation in tribocorrosive conditions, with the following objectives:

- Design and implement a sample holder bath as an integral component of the tribometer setup for conducting tribocorrosion tests. Simultaneously, utilise counter tips to replicate both single and multi-asperity contact, thereby facilitating idealized testing conditions in terms of environment, precision, and control.
- Investigate the influence of varying loads and potentials on wear and corrosion processes to clearly establishing their correlations on material degradation. This will involve assessing parameters including the Coefficient of Friction (CoF) and current measurements prior to, during, and after sliding.
- Leverage advanced interferometry and microscopy techniques like Vertical Scanning Interferometry (VSI) for surface topography and roughness measurement, Focused Ion Beam - Scanning Electron Microscopy (FIB-SEM) and Transmission Electron Microscopy (TEM), to capture high-resolution images of the wear scar and its microstructure. Additionally include a comprehensive assessment of the material's surface chemistry using Energy Dispersive X-ray Spectroscopy (EDX).

Chapter 2

2.1 Introduction

One of the most prevalent preclinical tests in both industry and research laboratories, with a focus on innovative bearing designs and materials for hip implants, is wear simulation [18]. Hip simulators are employed to replicate the biomechanics of human hip joints as observed in vivo, taking into consideration typical patient movements [19,20]. However, those tests predominantly provide wear rate data, offering limited insights into material responses to factors like load. In addition, those lacks a comprehensive understanding of smaller-scale wear mechanisms [21].

To advance implant designs and enhance implant longevity, a comprehensive comprehension of material behaviour is crucial. At the micron scale, a surface that may appear smooth in principle exhibits a rugged and uneven topography, characterized by asperities of varying heights and sizes. An example of such interface is shown in Figure 2.1. These asperities come into contact at diverse points, durations, and under varying stress conditions [22].

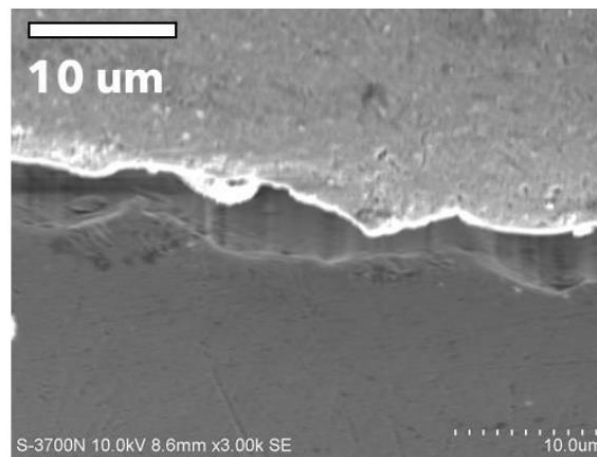


Figure 2.1. A scanning electron micrograph depicting a cross-section of a CoCrMo/Ti-6Al-4V head-neck modular taper following assembly and sectioning, revealing the asperity characteristics of the interface. It is essential to note that none of the interfaces observed in this image are in direct contact [22].

The advantage of utilizing micro scale tests stems from the fundamental role that the fracture of interlocking asperities plays during sliding contact. This fracture process significantly influences the levels of friction and wear experienced by brittle materials. The force required to break these surface asperities have a direct impact on factors like friction, wear rate, and how the surface roughness changes over time [18]. Furthermore, contacting asperities generate high contact pressures, which in turn instigate sub-surface alterations. In the case of CoCrMo alloys, the high-pressure conditions lead to strain accumulation at the contact interface. This strain fosters the development of a nanocrystalline microstructure within the material which than is subjected to wear due to the separation of nanograins, contributing to the overall degradation process [23,24].

2.2 Materials and methodology

In this section, we will delve into the materials used in our research. We will also detail the methodologies and techniques we employ to assess wear, corrosion, and the interplay between them. A schematic of the workflow is shown in Figure 2.2.

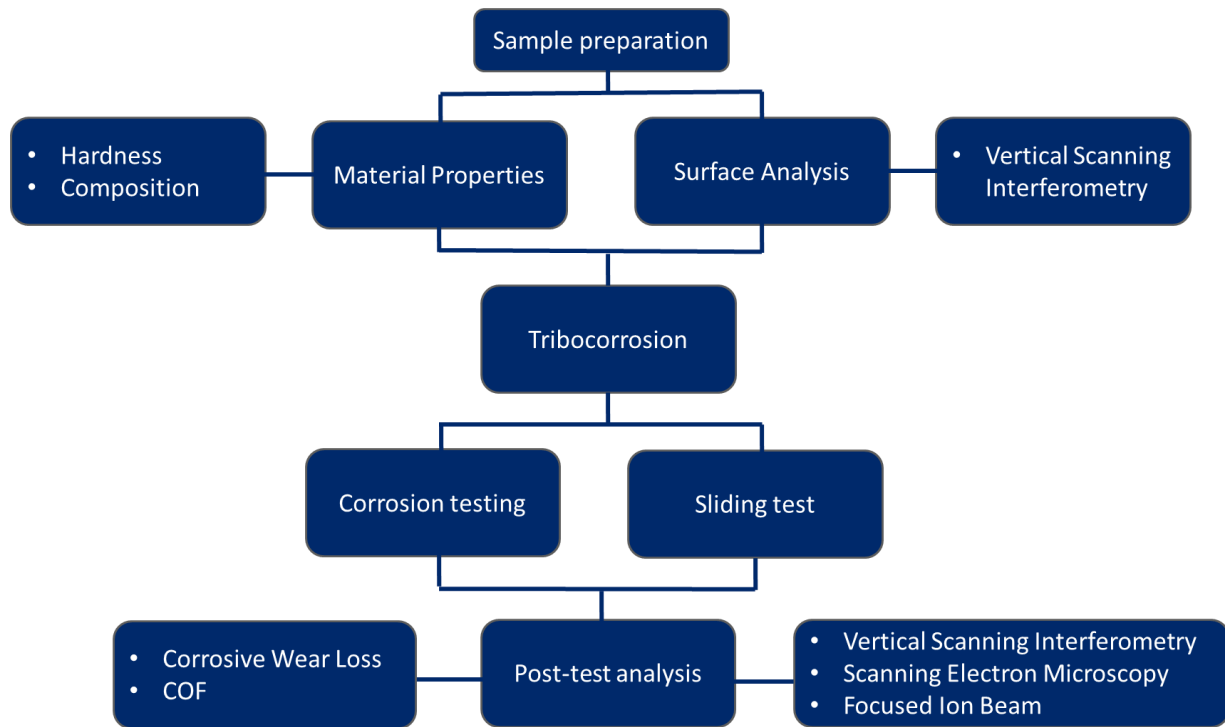


Figure 2.2 An experimental schematic showing the testing process from sample preparation to post analysis.

2.2.1 Materials

The examination focuses on evaluating low-carbon CoCrMo material as its breakdown products have held significance in influencing both cytotoxicity and clinical complications. This alloy is crafted in accordance with the specifications outlined in ASTM F1537.[25] The elemental composition of CoCrMo as per supplier’s (Oracle, UK) datasheet, conforming to the stipulations of the aforementioned standard, is delineated in Table 2.1.

Elements	C	Mn	Si	Co	Cr	Mo	Ni	Fe
Concentration (%)	0.23	0.70	0.70	61.29	29.60	6.40	0.10	0.64

Table 2.1. Composition of CoCrMo according to ASTM F1537

To facilitate testing, a 10 mm rod of low carbon CoCrMo is sectioned into 4 mm thick discs. These discs undergo a meticulous polishing regimen utilizing an Automated Polisher, commencing from a 600-grit level and progressively advancing to 4000 grit. Subsequently, a mirror finish is achieved through diamond suspension polishing up to $R_a \sim 5$ nm (Figure 2.3). To ensure uniformity across experimental conditions, the polishing process concludes prior to testing initiation. Following polishing, the samples undergo a thorough cleaning process according to ISO14242-2, involving a 10-minute immersion in an ultrasonic bath containing acetone, after which they are rinsed with deionised water and meticulously dried using an airgun.

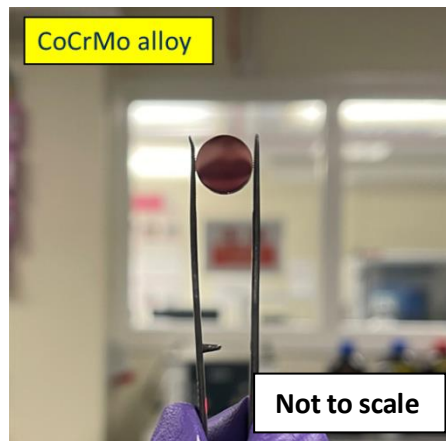


Figure 2.3. Mirror polished CoCrMo

To better understand how both small-scale (micro) and large-scale (macro) contacts contribute to wear formation, it's helpful to study how a controlled geometry of a single micro and macro contact interacts with a metal surface in tribocorrosive conditions. The tribological evaluation necessitates the employment of two distinct counter diamond tips (Micro Materials Ltd, UK) featuring a dome-shaped configuration (Figure 2.4). These tips are meticulously selected to mimic micro and macro -asperity contacts. To mimic a micro- asperity, contact a tip with a 25 μm diameter is chosen. A tip size of this magnitude has been previously documented in the literature for its ability to replicate a micro-contact asperity [26][27]. For similar reasons, it will be employed in this study.

In addition, a multi asperity macro-scale contact is mimicked with a diameter ten times bigger ($d=200\mu\text{m}$). The tip holder, constructed from Stainless Steel, encapsulates the diamond tips. To enhance isolation and eliminate ion release from the holder, a protective measure is adopted, entailing the application of an Acrylic Protective Lacquer layer (Electrolube, UK).

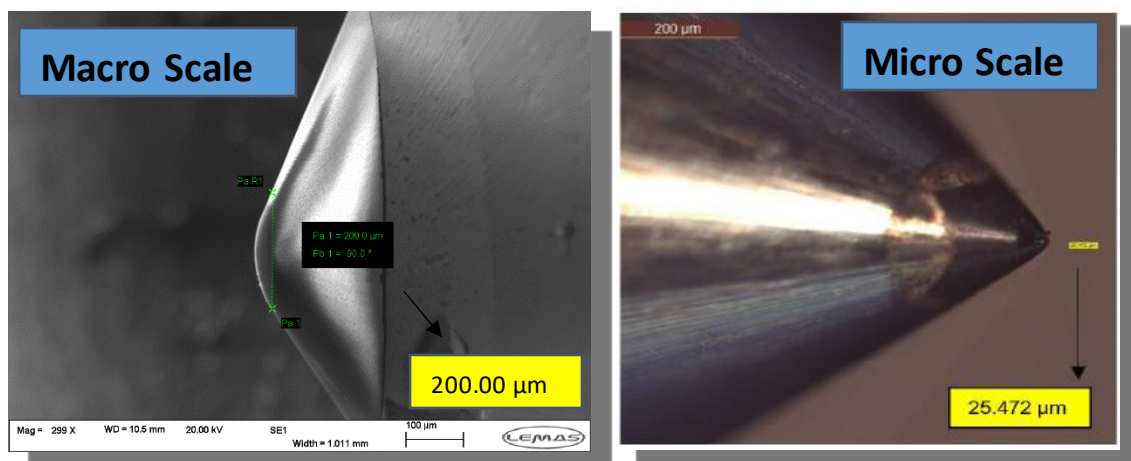


Figure 2.4. 200um and 25 um dome shaped diamond tip representing the macro and micro contact.

Phosphate buffer solution (PBS) (Thermo Scientific, UK) is prepared prior to the testing. In 100 mL ultra-pure water 1 tablet of commercially prepared PBS is dissolved using a magnetic stirrer. The buffer helps to maintain the pH (Using a pH probe the pH is measured $\text{pH}=7.25$). In addition, the ion concentration and osmolarity match that of a human body. The test initially is performed at room temperature to investigate only the impact of the microstructure on nano wear and ion release. The

same reason is applied for the chosen solution, as we do not want the content of the liquid to affect the film formation.

2.2.2 Methodology

In pursuit of deliverable D4.5 within the scope of the MSCA project, a series of tribocorrosion tests will be undertaken. The objective of these tests is to examine the consequences of single and multi-asperity scratch behaviours. This investigation will be executed utilizing the advanced capabilities of the Anton Paar NTR3 linear-reciprocating nanotribometer (as depicted in Figure 2.5), equipped with a High Load Cantilever (HL-S) designed to exert forces up to a maximum of 1 N. The NTR3 with an Atomic Force Microscopy (AFM) resolution offers exceptional precision in measuring nanoscale friction. It can measure forces in the nanonewton range, making it suitable for studying materials at very small scales.

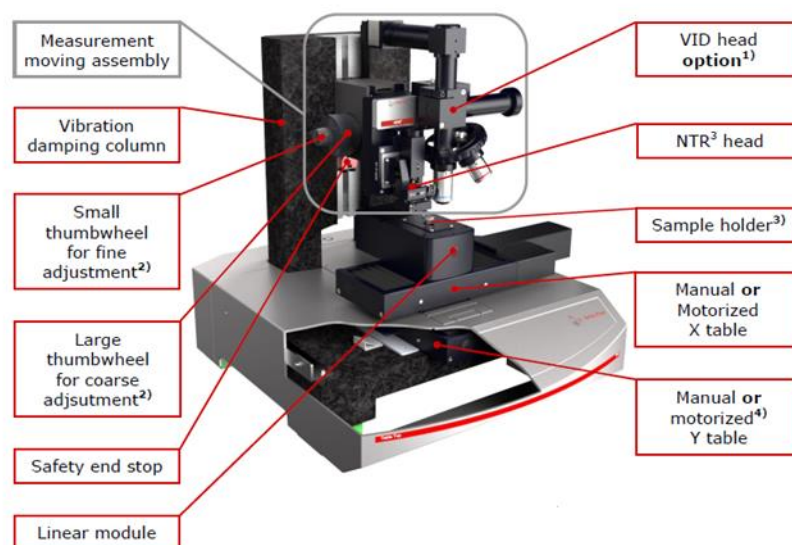


Figure 2.5. Schematic Representation of the Anton Paar NTR3 nanotribometer.

To dissect the influence of corrosion within sliding contexts, a new sample holder is devised (Figure 2.6) as an expansion to the nanotribometer framework. This component facilitates the immersion of samples in liquid, effectively mimicking in vivo conditions. The structural configuration encompasses an aluminium segment designated to accommodate the 10 mm sample specimen. Complementing this, a secondary component constructed from PEEK material is employed to secure and delineate the sample region to a dimension of 5 mm. The robust integrity of this system is further ensured through the incorporation of a dynamic sealing O-ring, effectively averting any unintended liquid leakage beyond the designated boundaries.

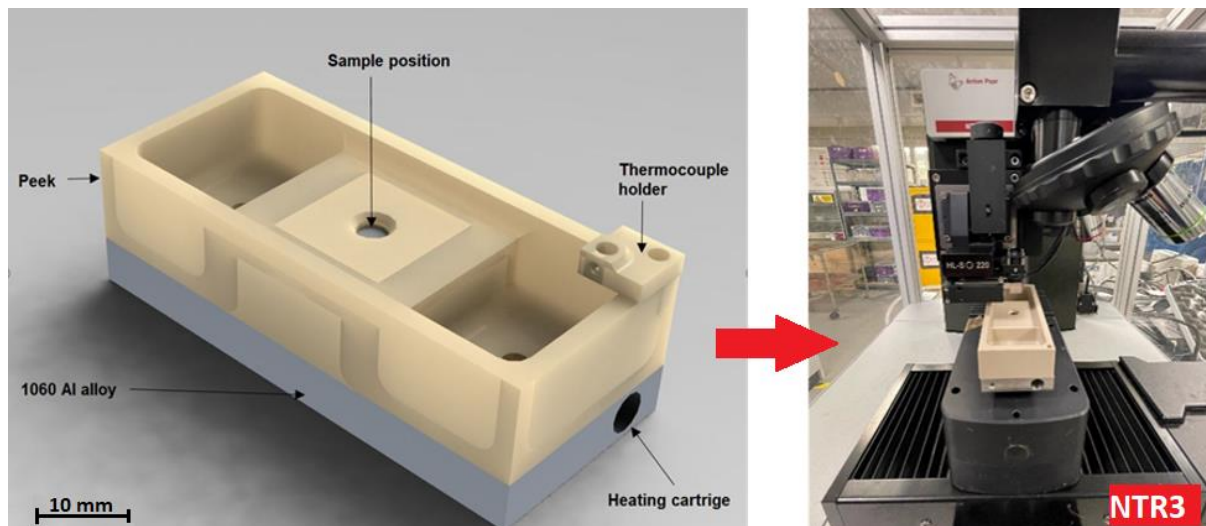


Figure 2.6 Sample holder for tribocorrosion testing secured in the NTR3 Tribometer.

To enable comprehensive electrochemical analysis, a three-electrode cell configuration is employed. This configuration integrates an Orion Redox ORP Electrode as the reference electrode with an included Platinum (Pt) counter electrode (ThermoFisher Scientific, UK). This electrode is situated within the solution. The Aluminium Sample Holder, which doubles as the working electrode, is electrically connected via a wire to facilitate electrochemical measurements. A schematic representation of the setup is shown in Figure 2.7.

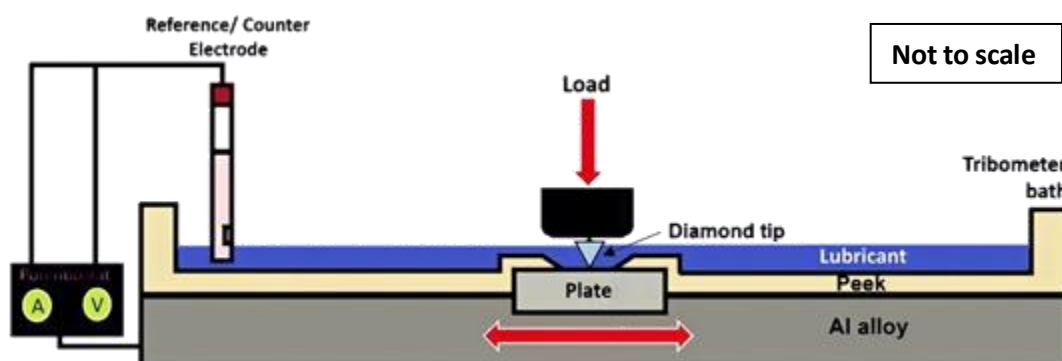


Figure 2.7. Schematic representation of tribocorrosion testing setup.

CoCrMo plates are tested under a wide range of loads namely 10 to 200mN corresponding to clinically relevant stresses. IviumSoft (Ivium Technologies, NL) is used for Chronoamperometry measurements.[15] A constant voltage of 0.1V is applied according to the baseline (For potential dependent testing this will vary to -0.8V, 0.1V and 0.2V with a static load of 200mN). Such amount has proven to shift the material into passivation region [28]. Prior sliding the current is left to stabilize for 30 minutes, with the load already applied. For simplified short testing the tip will scratch the surface for a sliding distance of 1.5 mm, while the Diamond tip will stay stationary. To be able to probe the currents at the nanoampere range a sliding speed of 1.5 Hz for a duration of 30 min is chosen. Those conditions are chosen to catch the scratching currents at the nanoampere region. The friction data, penetration depth and loads are recorded. Once the scratching of the surface stops the current is left to recover for another 30 min.

Using the mechanistic approach, the total wear volume loss is determined [29]. According to this method:

$$V_{total} = V_{chem} + V_{mech}$$

V_{total} is measured using profilometry (VSI) while V_{chem} in a potentiostatic tribocorrosion experiment can be determined from the measured current using Faraday's law:

$$V_{chem} = \frac{QM}{nF\rho}$$

Where Q is the electric charge flowing in the wear track obtained by integrating the measured current over the time of the experiment (Figure 2.8).

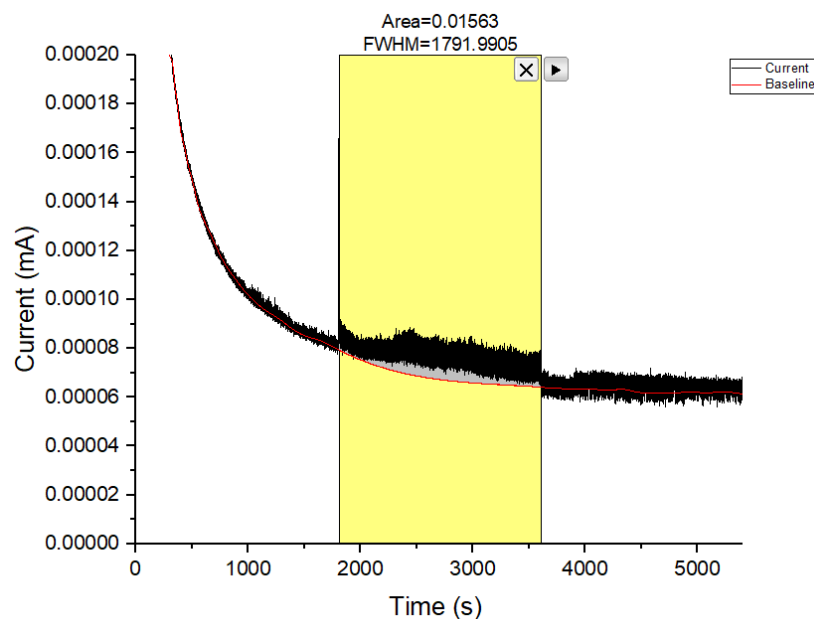


Figure 2.8. Current over Time graph showing an increased current during sliding. Area underneath the sliding current is equal to Q (electric charge).

2.2.3 Analysing equipment

Vertical Scanning Interferometer (VSI)

A Vertical Scanning Interferometer (VSI) is an optical instrument used for high-precision surface profiling and measurements. It involves the interaction of light waves to extract information about the surface being studied. For pre surface topographical measurements of the final mechanical polished CoCrMo surface a non-contact, white light interferometer (VSI, NPFlex TM, Bruker, US) is used. The main surface roughness parameter measured is S_a (arithmetic mean of asperities and plane). The same is subsequently employed to conduct a surface scan post-testing. Using VSI scans were carried out with a 10× magnification over an area of 1×1 mm². Three measurements were taken in different locations within 2.5 mm radius of the polished surface. Furthermore, the use of Vertical Scanning Interferometry (VSI) allowed for a thorough evaluation of the total volume loss. This is achieved by using Vison64 Software (Bruker, US) which precisely quantifies the changes in height across the entire surface area after sliding, providing quantitative insights into the amount of material that has been worn away.

Nanoindentation

The NanoTest NTX nano-indenter with a Berkovich type diamond indenter is used for hardness test. To begin, the sample is prepared. The sample should be flat and have a well-defined surface for testing. The NanoTest NTX is equipped with a sharp tip in the range of 20 to 100 nanometres, typically made of diamond. The tip is precisely positioned above the sample's surface. The instrument applies a controlled force or load to the tip, causing it to penetrate the surface of the sample. The depth of penetration is precisely controlled and monitored throughout the test. As the tip penetrates the material, it creates an indentation or impression on the surface. The depth of this indentation is a function of the applied load and the mechanical properties of the material. The NanoTest NTX typically follows a load-unload cycle. It gradually increases the load on the tip until a predetermined maximum load is reached and then decreases the load until it's back to zero. During both the loading and unloading phases, the instrument measures the force applied and the depth of penetration (Figure 2.9) [30]. After the test is complete, the collected data is analysed to determine various mechanical properties of the material. The key parameter for our test is hardness (resistance to plastic deformation). These properties provide insights into the material's mechanical behaviour at the nanoscale. To measure the hardness of the CoCrMo sample and achieve an average value, a matrix of 10 x 10 indentations in both x and y axis direction, were performed in the middle of the sample using load-controlled at 200mN. Assessing the hardness of a material near its surface holds significant importance in the context of conducting load-dependent tests as it provides vital insights into the material's resistance to plastic deformation and its ability to withstand localized stresses. Moreover, it allows us to link the materials microstructure changes and its wear behaviour when the initial surface pressures approach or exceed its surface hardness.

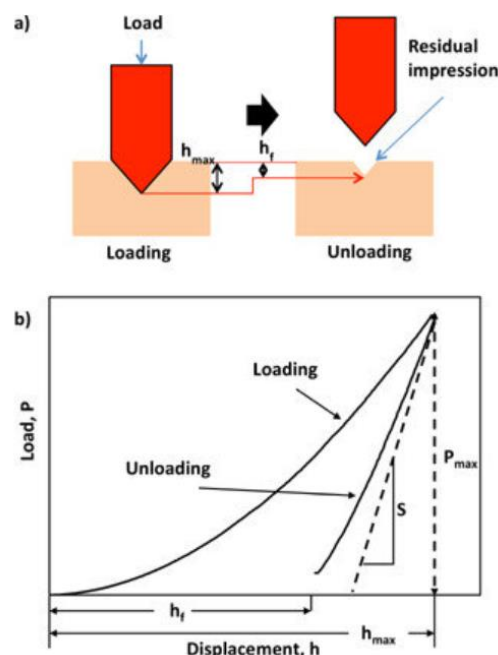


Figure 2.9. Nanoindentation illustration: (a) Schematic depicting the operational principles, and (b) a load-displacement graph illustrating the loading and unloading stages, with 'S' representing the contact stiffness during unloading. [30]

FIB-SEM

The Scanning Electron Microscope (SEM) is a pivotal tool in the realm of materials science and analysis, offering a means to investigate the morphological and structural characteristics of debris particles resulting from degradation processes. The FEI Helios G4 CX DualBeam used in this study is an advanced scientific instrument that combines capabilities of both a Scanning Electron Microscope (SEM) and a Focused Ion Beam (FIB) system.

The Helios G4 CX features an electron beam source, similar to a traditional SEM. It generates a focused beam of high-energy electrons using an electron gun, like a standard SEM. The electron beam is directed at the sample under investigation. When the electrons interact with the sample's surface, they produce various signals, including secondary electrons (SEs) and backscattered electrons (BSEs). The system is equipped with detectors to capture these signals. The secondary electron detector provides high-resolution images of the sample's surface topography, while the backscattered electron detector gives information about sample composition. In addition to SEM capabilities, the Helios G4 CX also includes a Focused Ion Beam (FIB) system. The FIB component of the instrument generates a focused beam of ions, typically gallium ions. Unlike electrons, ions can be used to mill or etch the sample's surface, which in this study is used for cross sections of the wear track for further microstructure analysis.

2.3 Summary

The current methodologies in preclinical testing for hip implants predominantly rely on joint simulators to evaluate wear rates. While these macroscopic tests offer valuable insights into the rate of material loss, they notably fall short in capturing the nuanced mechanisms contributing to overall material degradation. This limitation highlights a critical, yet unaddressed need for more in-depth studies at the microscale to elucidate the intricate interactions occurring at material interfaces.

To navigate this complexity, our research incorporates a comprehensive, multi-scalar approach that combines macroscopic and microscopic analyses. Within this framework, we employ idealized single and multi-asperity tests to scrutinize the surface interactions and microstructural changes that arise from the synergy between corrosion and mechanical wear.

To elevate the precision of our measurements and observations, we employ a state-of-the-art microtribometer. This allows us to probe the material properties at the microscale, yielding a granular understanding of tribological phenomena. This high-resolution analysis is further complemented by advanced microscopy techniques, which provide detailed characterizations of the material behaviour under varying tribocorrosive variables.

Through this integrated approach, our study aims to bridge the aforementioned gaps in implant material research, thereby offering a more complete picture of the mechanisms that govern material degradation. This deeper understanding is vital for advancing the field of hip implant design, and by extension, improving their long-term reliability and clinical outcomes.

Chapter 3

3.1 Introduction

In addition to the tribological assessments detailed in our study, it is pertinent to note that a critical aspect of our experimental protocol involves the preservation of lubricant samples from all tests. These collected lubricant samples have been meticulously frozen to maintain their integrity for subsequent debris analysis. This step allows us to gain further insights into the wear and degradation processes as well as their adverse effects.

ISO 17853 seeks to establish standardized procedures for isolating, evaluating, and describing debris. These techniques are designed to be reproducible and can be executed in a conventional laboratory setting. One limitation of the ISO standard is that it may discriminate against larger particles during the isolation process, potentially leading to incomplete isolation of smaller particles. While it suggests using higher centrifugal forces for longer durations to recover nanometre-sized debris, the standard does not provide specific guidelines for achieving this, leaving room for variability in practice. Furthermore, a study of Simoes et al. has proved that only centrifugation is not sufficient, in addition to it ultrafiltration is needed to separate nano wear and dissolved ions from the supernatant suspension [31]. This limitation highlights the need for clearer protocols to ensure consistent and comprehensive isolation of nanoparticles and ions. It's worth noting that neither ISO, ASTM, nor CEN currently encompass these elements as part of the degradation processes.

Furthermore, limitation of ISO 17853 is the lack of specific guidance on the removal of deposited debris from components. This omission poses a challenge as it may lead to the inadvertent release of particles into the lubricant during the isolation process, potentially resulting in an inaccurate representation of in vivo-generated debris. The absence of clear instructions for this crucial step impacts the precision and reliability of the standard's outcomes, emphasizing the need for further refinement in the methodology to ensure accurate characterization and assessment of particles. Yet another limitation of the ISO standard is its restriction to three particle shapes: round, oval, and needle (Table 3.1).

Aspect ratio	Shape
$1 \leq r < 1.5$	Round
$1.5 \leq r < 2.5$	Oval
$r \geq 2.5$	Needle

Table 3.1. Debris morphology categories according to ISO 17853.

Recent research, as demonstrated by authors such as Affatato et al. and Nine at al., has revealed the existence of additional particle categories, including aggregates (Figure 3.1) [32,33]. This discrepancy between the standard's prescribed categories and emerging research findings underscores the need for the standard to evolve and encompass a broader range of particle shapes to accurately capture

the diverse nature of debris in real-world scenarios. Different shapes and sizes were listed by the ASTM F1877-16 however without providing a standardized quantifying method to distinguish between them.

While ASTM standards offer a comprehensive classification system for particles, the absence

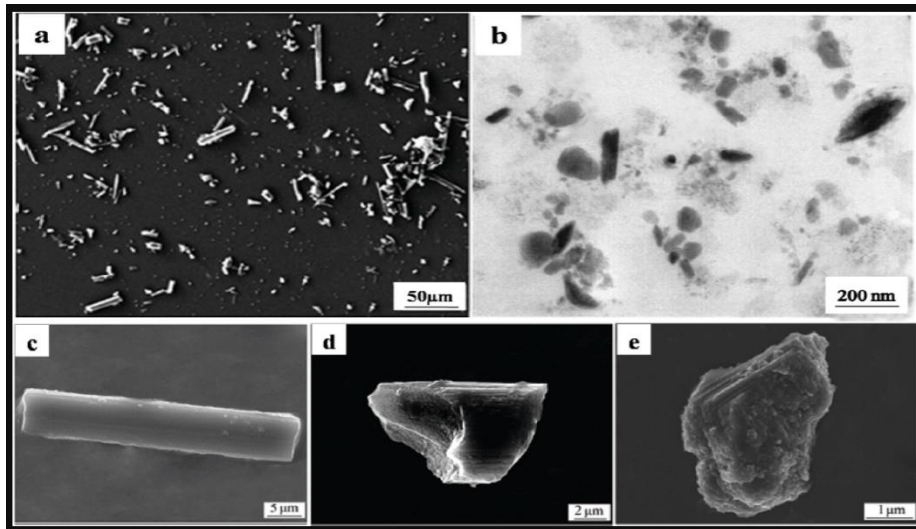


Figure 3.1. Common morphological forms of debris derived from joint simulators include: (a) Carbon-Carbon (C/C) composites; (b) Chromium-Cobalt (CrCo) alloy; (c) Cylindrical shapes specifically within C/C composites; (d) Radially fractured forms also within C/C composites; and (e) Block-like or sliced configurations again within the realm of C/C composites.[31]

of clear quantification criteria hinders the practical application and consistency of these categories.

Another methodology for isolation of debris is the one from the CEN Workshop Agreement. With the above limitations in mind, the Cen Methodology is adept at capturing particles of all sizes, thereby providing a more comprehensive view of the debris generated. This is crucial for understanding the full scope of wear and degradation mechanisms at play. Having in mind that our testing's are run at the microscale using a single asperity approach the above methodology is equally effective at isolating smaller volumes of debris. A significant advantage of the CEN Methodology for Debris Isolation is its elevated yield, surpassing conventional techniques. High yield is paramount for obtaining a statistically meaningful sample size, which in turn ensures the robustness of subsequent analyses. This is especially crucial in studies where the volume of generated debris is inherently low and each particle holds critical information about the wear and corrosion processes, making this method more ideal for debris isolation. Besides size and morphology another important factor is the degradation of the debris with time. Simoes et al., has further extended debris analysis and understand their morphology changes by utilizing an ex-situ static corrosion in different pH environments [31]. The methodology focuses on the examination of the debris in normal and inflammatory conditions allowing for a comprehensive examination of the debris interactions with the surrounding medium. It also contributes to a comprehensive understanding of the potential consequences of these particles when they are introduced into various contexts.

3.2 Aims and Objectives

The primary aim of this research segment is to characterize debris and ion release originating from previous tribocorrosion tests. Furthermore, link their characteristics to the degradation mechanisms

outlined in Chapter 2. This integrated approach seeks to overcome the limitations of existing standards, thereby enabling more comprehensive and reliable assessments.

- **Debris Characterization:** To utilize a synthesized protocol, incorporating elements from CEN Workshop Agreement, for the detailed characterization of debris from prior tribocorrosion tests. And including methodologies by Simoes et al., for the accurate quantification and assessment of metallic ions released during tribocorrosion processes.
- **Load and Potential Correlation:** To establish empirical relationships between varying mechanical loads and electrochemical potentials, and their subsequent effects on debris morphology and ion release patterns.
- **Environmental Assessment:** To extend the utility of the synthesized protocol to ex situ assessments of debris in diverse media and corrosive environments, facilitating a more comprehensive understanding of debris and ion interaction under different conditions.

These objectives offer a structured approach to investigate the intricate relationships between tribocorrosive mechanisms and debris characteristics, providing both depth and reliability to the study.

3.3 Methodology

To accurately measure the debris and ions produced in total hip arthroplasty (THA), a process involving isolation, evaluation, and characterization is necessary. This section provides an overview of established techniques for isolating debris from test fluids utilized in laboratory testing, prevalent analysis methods for evaluating debris and ions. The following methodology according to the CEN Workshop Agreement is used for isolating metallic debris from PBS in combination with Simoes et. al methodology for ICP-MS for metallic trace analysis ex situ. This is recommended as it will remove impurities, dust and other substances that may have fallen into the lubricant over time. A detailed

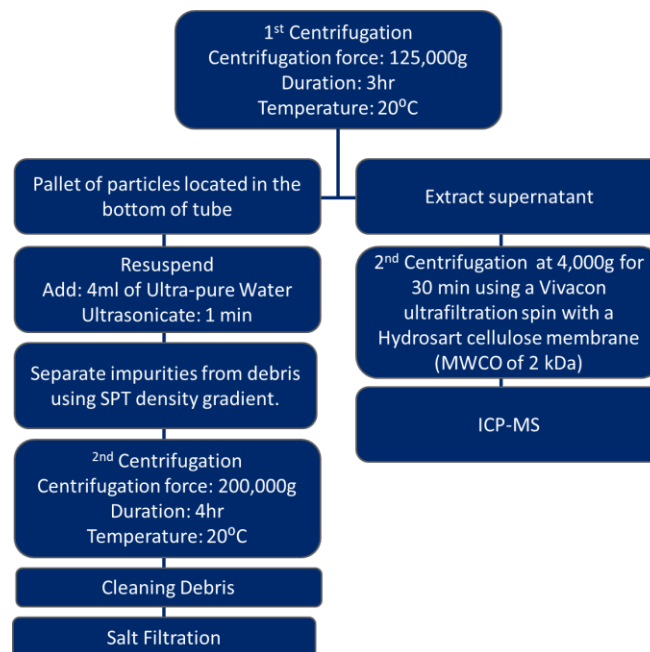


Figure 1.2 A schematic on the workflow for particle isolation and sample preparation for metallic trace analysis.

schematic is shown in Figure 3.2.

3.3.1 Debris Isolation

In the methodology, should the post testing lubricant be in a frozen state, we employ a rapid thawing technique. This is accomplished by introducing the cryogenically preserved specimen into a receptacle containing warm water with a temperature maintained below 35°C or by subjecting it to a heated ultrasonic bath also maintained below 35°C. If a decrease in temperature occurs during the thawing process, the addition of warm water is permissible to expedite the process. To aid in the thawing procedure, the specimen is agitated at intervals of 10 minutes. Once the lubricant reaches ambient temperature post-thawing, we promptly initiate the isolation procedure. However, in cases where the lubricant remains unfrozen, and the analysis is conducted immediately following the sliding test, this procedural step of thawing is omitted.

After defrosting the total sample is subsequently divided into individual tubes, and ultrapure water is added to each tube until all tubes attain an equal mass, typically aiming for a total mass (tube + cap + sample + water) of 50.00 g \pm 0.01 g. While precision to exactly 50 g is not mandatory, maintaining equal weight among tubes and ensuring they are filled above 60% capacity is essential. Subsequently, each tube is carefully placed into the centrifuge and subjected to a centrifugal force of 125,000g for a duration of 3 hours at a temperature of 20°C. During this centrifugation process, each tube generates a pellet of particles located at the bottom. To proceed, the supernatant, which is the liquid portion above the pellet, is meticulously extracted from the sample using a pipette. Particular attention is paid to preserving the integrity of the pellet. The extracted supernatant is promptly frozen for later use in ion analysis, as elaborated upon in subsequent sections of this document, particularly in section 3.3.4.

Following the centrifugation step, the pellet within each ultracentrifuge tube is resuspended to eliminate impurities effectively. To achieve this, 4 ml of ultrapure water is carefully introduced into each tube. Subsequently, the tube is placed in an ultrasonic bath for a duration of 1 minute. Simultaneously, a glass rod is employed to gently stir the contents, facilitating the suspension process, and ensuring that the pellet is thoroughly resuspended in the solution. This meticulous resuspension step is crucial for further analysis and characterization of the debris particles.

Continuing with the procedure, this step serves to effectively separate impurities from the debris. To achieve this separation, we utilize an SPT (sodium polytungstate) density gradient, exploiting the differential buoyant densities of impurities and debris. During centrifugation, impurities will migrate upward through the gradient, while debris particles will remain concentrated at the bottom.

In a dedicated ultracentrifuge tube, a layering process is initiated, with 2 ml of each of the following SPT solutions sequentially added: 1.8 g/ml SPT, 1.6 g/ml SPT, 1.2 g/ml SPT. This precise layering of SPT solutions establishes a density gradient within the tube, creating the conditions necessary for effective separation and isolation of the debris particles from impurities during subsequent centrifugation.

After the preparation of the SPT gradient, the test sample, containing the debris solution, is subjected to agitation for a duration of 10 minutes within an ice-cooled ultrasonic bath. It is essential to handle this step with care to ensure thorough mixing of the sample while avoiding disruption to the established density gradient. Subsequently, 4 ml of the debris solution is carefully pipetted from the test sample and added to the top of each ultracentrifuge tube.

To ensure uniformity and equal mass among the tubes, ultrapure water is added to each tube, typically aiming for a total mass (tubes + cap + sample + gradient + water) of 50.00g \pm 0.01 g. Although exact precision to 50 g is not mandatory, maintaining equal weight among the tubes and ensuring they

are filled above 60% capacity is here essential as well. The prepared ultracentrifuge tubes are then placed within the ultracentrifuge and subjected to centrifugation for a duration of 4 hours at a force of 200,000g and a temperature of 20°C. This centrifugation process will result in the formation of a debris pellet located at the bottom of the tube, with impurities positioned higher up within the tube. This separation is critical for the subsequent analysis and characterization of the isolated debris particles.

Cleaning debris

In the methodology, the isolated debris are cleaned by separating them from impurities and the SPT density gradient. This purification process involves several iterations. Initially, 10.5 ml of liquid from each tube is carefully removed and discarded, effectively eliminating impurities and excess SPT. Subsequently, 5 ml of ultrapure water is added to each tube, and they are placed in an ultrasonic bath maintained at 50°C for 1 minute. During this period, a glass rod is employed to gently break up the debris pellet, aiding in its resuspension. To ensure uniformity among the tubes, they are topped up with ultrapure water to achieve a total mass (tubes + cap + sample + water) of approximately 50.00 g \pm 0.01 g. Following this, the tubes are stirred, and then they are placed in the ultracentrifuge for 1 hour at a temperature of 30°C and a force of 125,000g. This cleaning procedure is repeated three times in total, with each repetition involving the removal of 10.5 ml of liquid, the addition of 3 ml of ultrapure water, 1 minute of sonication, topping up with ultrapure water for equal weight, and subsequent centrifugation for 1 hour at 125,000g. As the final step in the methodology, the cleaned debris should now be found in the form of a clean pellet settled at the base of the tube.

To proceed, most of the liquid within the tube, approximately 95%, is carefully removed, with utmost caution taken to avoid disturbing the debris pellet during this process. To resuspend the debris, 5 ml of ultra-pure water is introduced into the tube, and the mixture is subjected to sonication while concurrently stirring with a glass rod.

In addition to that because of the high content of salt in PBS a 20 nm Anodisc Inorganic Filter (Whatman, UK) is used to separate the salts from the debris. These meticulous steps are undertaken to ensure the thorough separation of debris from impurities, resulting in a purified debris sample suitable for further analysis.

Finally, the prepared debris samples are securely frozen until they are required for subsequent usage in further experiments and analyses. After isolation, thorough assessment of the debris can be conducted through various methodologies.

3.3.4 Methodology for preparation of ICP-MS for metallic trace analysis

This report details the step-by-step approach for preparing samples for trace metal ion analysis using the ICP-MS technique as described by Simoes et al. Given that our sample is devoid of protein content, the protein digestion steps delineated in Simoes et al. will be omitted from our experimental procedure [31].

From the supernatant taken from the first isolation step explained in chapter 2.2 an additional centrifugation step at 14,500 rpm (equivalent to 14,000g) for 30 minutes is carried out. This centrifugation is carried out using a Vivacon ultrafiltration spin column that is equipped with a Hydrosart cellulose membrane with a molecular weight cut-off (MWCO) of 2 kDa. This MWCO roughly corresponds to a pore size of approximately 1.5 nm.

Then the samples underwent a secondary centrifugation step at 14,000 rpm for 10 minutes, after which 0.5 ml of the resulting supernatant is collected and subsequently diluted in 8 ml of MilliQ

Water. Finally, the quantification of isotopes ^{59}Co , ^{52}Cr , and ^{96}Mo is conducted through the utilization of Inductively Coupled Plasma Mass Spectrometry (ICP-MS).

3.3.5 Static corrosion ex-situ

Upon successful isolation of particles from the initial solution, the filters are simply immersed for 24 hr and resuspended in three distinct media: Human Plasma Like Medium (HPLM), and Bovine Serum Albumin (BSA). This variation in suspending media is designed to simulate a range of biologically relevant environments, thereby offering insights into the behaviour of the particles under different conditions.

Initial static dissolution studies, or incubation, will be conducted at a temperature of 37°C and a pH of 7 for a duration of 24 hours, at 1V to shift the material into the corrosion regime. This phase aims to replicate physiological conditions, providing preliminary data on the dissolution behaviour of the particles.

To further our understanding of the particles' long-term behaviour, additional incubation studies will be carried out over extended durations of 1, 3, and 6 months. These studies will be performed at a lower temperature range of $3\text{-}4^{\circ}\text{C}$, intentionally avoiding temperatures that are conducive for bacterial growth. This allows for the assessment of particle stability and potential transformations without the confounding variable of microbial contamination.

3.3.5 Equipment

Scanning Electron Microscopy (SEM)

Particle images will be acquired utilizing a Hitachi HRSEM, with sampling at five distinct locations as delineated in Figure 3.3. To achieve a comprehensive view, five varying magnifications will be applied, specifically $\times 1,000$, $\times 5,000$, $\times 10,000$, $\times 50,000$, and $\times 100,000$. To mitigate the issue of charging, a carbon coating will be applied to the samples. In addition to second electron imaging backscattered electron (BSE) techniques will be employed. Subsequent image analysis will be conducted using Image J (National Institutes of Health, US) software to evaluate particle size and shape. The particle size distribution will be both plotted and reported in both normal and logarithmic scales, incorporating parameters such as particle height and width. Each analytical test will encompass the study of 100 particles. For elemental characterization, energy-dispersive X-ray spectroscopy (EDX) will be utilized to detect trace elements.

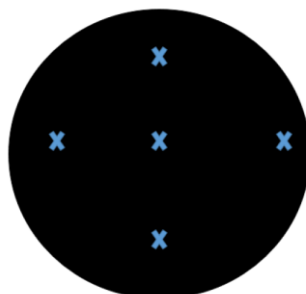


Figure 3.3. SEM Imaging points

In the process of image analysis, the scale is initially set to ensure accurate dimensional measurements, typically expressed in terms of pixels per unit distance. Following scale calibration, the image is converted to an 8-bit grayscale format to enable efficient threshold adjustment. Subsequently, the threshold settings are fine-tuned to segregate the particles from the background, a crucial prerequisite for subsequent segmentation. A specific region of interest (ROI) within the image is then selected for focused analysis. The thresholded image is converted into a binary format, and denoising algorithms are applied to minimize image noise and enhance the quality of particle segmentation. Edge-detection algorithms are employed to outline the individual particles within the binary image, thereby isolating each for subsequent analysis. Finally, particle analysis algorithms are invoked to extract pertinent metrics such as size, shape, and distribution, which are then recorded for further analysis and interpretation.

Transmission Electron Microscope (TEM)

Transmission Electron Microscopy (TEM) constitutes an indispensable technique for the meticulous investigation of debris particles. This method revolves around the passage of a focused electron beam through a thinly sectioned sample. The interactions between the electron beam and the sample give rise to diffraction patterns and image contrasts that unveil intricate details regarding the particles' internal structure, crystallography, and elemental composition. Unlike SEM, TEM can achieve exceptionally high magnifications, upwards of 50,000,000 times, permitting the discernment of minute features at the nanometre scale. It is imperative to note that TEM demands specimens of extreme thinness, typically less than 150 nm, due to the limited penetration depth of the electron beam. This stipulation restricts its application to solid samples.

Atomic Force Microscope (AFM)

The Atomic Force Microscope (AFM) stands as a versatile tool in the realm of surface analysis, endowing researchers with the ability to discern three-dimensional topographical characteristics of debris particles. AFM operates by employing a microfabricated cantilever tipped with a sharp apex that is raster-scanned across the sample's surface. The interaction forces between the tip and the sample cause the cantilever to deflect, and this deflection is detected and transformed into a topographic image. AFM is notable for its capacity to scrutinize various sample types, ranging from hard materials to biological specimens, with high lateral resolution. However, AFM's depth profiling capabilities are constrained by its relatively shallow scanning depth, typically confined to 5 – 6 μm , making it more suited for the analysis of surface features.

Dynamic Light Scattering (DLS)

Dynamic Light Scattering (DLS) is an invaluable technique harnessed for the determination of particle size distributions in liquid suspensions. Rooted in the principle of Brownian motion, DLS monitors the fluctuating intensity of scattered light as particles undergo random movement due to interactions with surrounding solvent molecules. Larger particles exhibit slower Brownian motion compared to smaller particles, leading to distinct scattering behaviours. By analysing the temporal fluctuations in scattered light, valuable insights into particle sizes within the nanometre to micrometre range can be garnered. It is crucial to maintain highly diluted particle suspensions and a constant knowledge of liquid viscosity and temperature. DLS excels in capturing sizing information for larger volumes of debris, although it does not provide details about particle morphology.

3.4 Summary

Our investigation extends beyond tribological assessments to include a rigorous protocol for the isolation and analysis of lubricant samples. Linking mechanical load and electrochemical potentials to the morphology and composition of tribocorrosive debris enhance the scope and reliability of our tribological assessments. While the ISO standard ensures a degree of reproducibility, it suffers from multiple limitations. These include the imprecise isolation of nanoparticles, neglect ions release, unclear instructions for the removal of deposited debris, and a limited scope for categorising particle shapes. Alternative methodologies, such as those of the CEN Workshop Agreement, are therefore considered for their higher yield and more comprehensive particle size capture. This alternative methodology has further been extended by incorporating steps to remove additional salts left by the supernatant by using filtration, methodologies by Simoes et. al for precise measurements of metallic ions, as well as preparing debris appropriately for later cell studies.

Moreover, our study extends the existing paradigm by including ex situ assessments of how debris reacts in various media and corrosive environments, augmenting our understanding of how debris morphology changes over time and under different variables. This offers a more holistic understanding of debris interactions and the potential ramifications when introduced into various settings.

In conclusion, our study addresses a crucial gap in the current scientific literature concerning tribocorrosive phenomena and debris characterization. Through the adaptation and amalgamation of various methodologies, we have created a robust framework capable of not only identifying and isolating debris but also understanding its interactions in different environments. Our work thus contributes to the foundational knowledge in the field and suggests a path for future investigations aimed at the comprehensive understanding of tribocorrosion and its consequences.

Chapter 4

4.1 In situ degradation methods for nanoparticles

In CoCrMo alloys, stability is generally maintained through a chromium oxide-based passive layer that inhibits the release of ions. However, under elevated electrochemical potentials, particularly within biological systems, this passive layer is prone to failure, resulting in the potential liberation of toxic ions [34]. It is well known that cobalt ions (Co(II)) exhibit both cytotoxic and genotoxic properties [35,36]. Another critical yet unresolved clinical issue pertains to the in vivo breakdown mechanism of CoCrMo, a material generally considered stable. Moreover compounds of chromium in the Cr(VI) oxidation state are recognized as carcinogenic [37]. This has elicited considerable clinical concern, especially given the high levels of Co dissolution observed in vivo. Consequently, to elucidate the in vivo degradation mechanisms of CoCrMo particles, high-resolution and in situ analyses remain imperative.

To understand the behaviour of CoCrMo particles a few studies have been conducted. In the study of Mohammed et al., both ex situ and in situ electrochemical tests were performed to examine the behaviour of CoCrMo wear particles in simulated body fluid (SBF), an environment that mimics macrophage cells [38]. Two in situ methods were employed for analysis. The first, using Diamond Beamline I20. The second method, conducted at SSRL Beamline 6-2, utilized a 3D-printed electrochemical cell for in situ imaging. Transmission X-ray Microscopy (TXM) was used to observe initial morphological changes in CoCrMo particles [38]. Similarly, Koronfel et al. used the same methodology to enable real-time observation, providing insights into the dynamics of Co and Cr dissolution [39].

Overall, the integration of TXM-XAS holds significant promise for the comprehensive analysis of nanoparticle morphological evolution in our forthcoming research. The approach offers distinct yet complementary capabilities for characterizing structural and compositional changes, thus enriching the dataset, and enhancing the robustness of our investigative framework.

4.2 Aims and Objectives

Building upon our existing work on debris formation and characterization, this part of the methodology aims to investigate the in-situ degradation of nanoparticles. This endeavour will furnish the requisite data to form a comprehensive and nuanced understanding of the degradation processes, encompassing the full trajectory from wear formation to particle evolution.

The objectives for the in-situ study are:

- Observe and quantify the real-time dissolution kinetics of Co and Cr elements from CoCrMo nanoparticles under controlled electrochemical conditions.
- To employ in situ X-ray absorption spectroscopy (XAS) at specified photon energies to monitor elemental-specific fluorescence signals, thereby tracking dissolution rates and compositional alterations.
- To capture Transmission X-ray Microscopy (TXM) images to elucidate the onset of morphological transformations in nanoparticles as they undergo electrochemical reactions.

- To assess and quantify any transient presence of Cr(VI) species as part of the study into Cr speciation during nanoparticle dissolution.

By addressing these objectives, the study aims to provide a detailed in situ account of nanoparticle evolution, contributing to a broader understanding of their behaviour in complex electrochemical systems.

4.3 Equipment and Methodology

4.3.1 Equipment

Transmission X-ray Microscopy coupled with X-ray Absorption Spectroscopy (TXM-XAS) is a powerful analytical technique for investigating the spatial distribution of elements and their chemical states at the nanoscale [40]. The method combines the high-resolution imaging capabilities of transmission X-ray microscopy (TXM) with the element-specific chemical analysis provided by X-ray absorption spectroscopy (XAS) [41]. In TXM, X-rays are focused onto the sample, and an image is formed based on the transmitted X-rays, similar to how a standard microscope works with visible light. This allows researchers to obtain high-resolution spatial information about the sample, typically with resolutions on the order of tens of nanometres [40].

The coupling of TXM with XAS allows for a more nuanced investigation. XAS provides information on the oxidation state, local geometry, and electronic structure of the targeted element within the sample. By combining these two techniques, it's possible to map these chemical properties across the spatial architecture of a sample. This is particularly useful for heterogeneous materials, catalysts, or biological samples where understanding the relationship between structure and function is critical [40,41].

TXM-XAS is often used in situ, meaning it can analyse a sample under conditions that closely mimic its natural or operational environment. This is critical for time-resolved studies where changes in chemical state or structure over time are of interest. However, it's worth noting that the selection of photon energies for the XAS part is a trade-off. Higher resolution in energy allows for more accurate chemical identification but may require longer acquisition times, which could be a limitation for studying fast dynamic processes.

4.3.2 Methodology

The following methodology is based on the Imperial approach on in situ nanoparticles analysis [38,39], but has been modified as per our needs, including the change of media and light source used. Isolated particles are initially stored in isopropyl alcohol at 4°C before use, these suspensions are sonicated and then drop-cast onto an 8- μm -thick gold-coated Kapton film, which subsequently undergoes drying in a low-temperature vacuum oven. The gold layer serves as the working electrode for applying electrochemical potentials to CoCrMo particles [38,39].

In our study those particles will be investigated under different media including PBS, HPLM and BSA. For Co speciation, a sophisticated setup at the Diamond Synchrotron Radiation Lightsource (SSRL), UK is used. Electrochemical potentials are applied in 400-second steps, in a range of 0.4 to 0.8 V. Transmission X-ray microscopy (TXM) with multiple energies is used to obtain detailed absorbance images and X-ray Absorption Spectroscopy (XAS) data for the CoCrMo particles. Six incident photon energies are carefully chosen for imaging to balance between the need for accurate chemical analysis and temporal resolution. The first three energies, namely 7659, 7679, and 7699 eV, serve to remove spectral background. The next two energies, 7710 and 7727 eV, are critical for differentiating chemical species. The final energy selected is 7788 eV, an isosbestic point used for normalizing all data; this energy relates to the total Co content without regard to its chemical state [38,39].

Cr speciation studies aim to identify the onset of Cr(VI) release. In the Conventional X-ray Absorption Spectroscopy (XAS) approach, a large beam size of 1 mm × 9 mm is used to measure the absorbance intensity of Cr(VI) over time and varying potentials. The study employs a fine temporal resolution of 0.33 seconds. A Cr(VI) standard is used to determine the pre-edge peak energy at 5993.25 eV. Additional time scans at 6009 eV are conducted. Electrochemical conditions include an initial 5-minute open-circuit potential (OCP), 75 minutes of stepped potentials from 0.4 to 0.8 V, and a concluding 20-minute OCP. The OCP values shift from -70 mV before to 450 mV after the applied potentials. Moreover, X-ray Absorption Near Edge Structure (XANES) spectra are recorded at different instances: before and after the addition of electrolyte, post application of potential steps, and from samples detached post-bias. This methodology offers a nuanced understanding of Cr speciation and electrochemical behaviour in CoCrMo thin films [38,39].

4.4 Summary

The research provides an in-depth exploration of CoCrMo alloy particles, focusing on their degradation mechanisms, particularly in situ. These alloys generally rely on a passive chromium oxide layer for stability, which is prone to failure under certain electrochemical conditions, leading to the release of potentially toxic cobalt and chromium ions [38]. Two advanced techniques, namely Transmission X-ray Microscopy (TXM) and X-ray Absorption Spectroscopy (XAS), were employed in an integrated manner for the in-situ analysis of these particles. This methodological framework, which also included specific setup configurations for Cobalt and Chromium speciation, allowed the study to achieve its objectives. These objectives ranged from real-time observation of dissolution kinetics to capturing morphological changes and tracking compositional alterations.

The study substantially advances our understanding of CoCrMo particle degradation. Employing an integrated TXM-XAS approach has proven to be invaluable for characterizing both structural and compositional changes at the nanoscale. This comprehensive method has not only fulfilled the study's immediate objectives but also holds promise for further research, given its capacity for real-time, in situ analyses. By addressing both the kinetics of Co and Cr dissolution and the transient presence of Cr(VI) species, the study contributes significantly to the broader understanding of the behaviour of nanoparticles in the complex in vivo environment. Furthermore, this work has the potential to influence future regulatory guidelines, aiming to improve the safety and efficacy of implantable devices.

Chapter 5

5.1 Discussion and Conclusion

5.1.1 Discussion

Our study presents a comprehensive approach, spanning from the inception of wear formation mechanisms to debris analysis and further the subsequent exploration of cell interactions, which will be outlined in Deliverable 4.6. This multifaceted investigation seeks to address the intricate aspects of implant degradation, offering valuable insights into the entire process.

Our approach builds upon and extends the seminal work of Wimmer et al. and Fischer et al., who focused on microstructure changes [15-16], but within the context of a tribocorrosive environment. Additionally, our research advances the work of Gilbert et al. [17] by incorporating idealized single and multi asperity stretching from the micro to the macro scale wear formation and connecting it to tribological phenomena. This amalgamation of methodologies allows us to unravel the complexities of debris formation at a finer scale, ultimately enhancing our understanding of the processes involved.

Furthermore, our methodology includes a crucial step of debris isolation, where we employ the CEN Workshop agreement in combination with the methodology by Simoes et al. [31]. The combined methodology represents a notable refinement compared to the ISO 17853 and ASTM F1877-16 standards. The CEN Workshop agreement not only enables the capture of nanometric-sized debris but also allows for the precise characterization of their morphology with a high yield. While Simoes et al. provides a comprehensive protocol for the effective separation of ions from the supernatant for metallic trace analysis.

Besides the morphological characterization, and release of metallic ions we conduct ex situ corrosion tests on the isolated debris, following the approach demonstrated by Simoes et al. in Chapter 2 [31]. These tests serve to elucidate the changes in chemical composition and morphology of the debris over time, offering valuable insights into their evolution.

To culminate our investigation, we employ in situ testing methods, drawing upon the Imperial techniques [38,39]. This final step affords us a comprehensive understanding of the degradation of CoCrMo debris under realistic conditions, bridging the gap between laboratory-controlled experiments and real-world scenarios.

The utility of a multi-methodological analysis in elucidating the origins, properties, and mechanisms of debris degradation and ion release is crucial. Notably, such an integrated methodological approach has neither been previously documented nor incorporated into extant regulatory assessments. A comprehensive grasp of these degradation processes could catalyze meaningful advancements in the design of implant materials, thereby attenuating health risks such as toxicity and carcinogenicity.

5.1.2 Conclusion

In conclusion, our research workflow represents a holistic and integrated approach to the analysis of implant degradation, addressing existing gaps in the field. Our study encompasses the entire spectrum, from wear formation mechanisms to debris analysis, and further delves into cell interactions, providing a comprehensive understanding of this intricate process. By employing an idealized tribocorrosive single asperity model, we extend the current state of knowledge, elucidating the mechanisms of debris formation at a microscale level.

The incorporation of advanced techniques, such as the CEN Workshop agreement for debris isolation and characterization, adds a layer of precision and sophistication to our research. Furthermore, our work includes ex situ corrosion tests to track the chemical and morphological changes in debris over time. Finally, in situ testing using the Imperial methods provides a realistic assessment of debris degradation under actual conditions.

In this study we have chosen the most comprehensive and meticulous approach to form a solid foundation for understanding implant degradation and paves the way for the development of more resilient implant materials and enhanced biomedical applications. Our research endeavours to contribute significantly to the field, offering a detailed and integrated perspective on implant degradation processes.

References

- [1] R. Pourzal, I. Catelas, R. Theissmann, C. Kaddick, A. Fischer, *Wear* 271 (2011) 1658–1666.
- [2] P.K. Chu, J.Y. Chen, L.P. Wang, N. Huang, *Mater. Sci. Eng. R Reports* 36 (2002) 143–206.
- [3] X.-W. Liu, Y. Zi, L.-B. Xiang, Y. Wang, *Int. J. Clin. Exp. Med.* 8 (2015) 27–36.
- [4] J.T. Evans, J.P. Evans, R.W. Walker, A.W. Blom, M.R. Whitehouse, A. Sayers, *Lancet* 393 (2019) 647–654.
- [5] E. Lenguerrand, M.R. Whitehouse, A.D. Beswick, S.A. Jones, M.L. Porter, A.W. Blom*, *Bone Joint Res.* 6 (2017) 391–398.
- [6] Y. Yan, A. Neville, J. Hesketh, D. Dowson, *Tribol. Int.* 63 (2013) 115–122.

- [7] D. Bitar, *World J. Orthop.* 6 (2015) 172.
- [8] Off. J. Eur. Union (2017).
- [9] E. Thienpont, G. Quaglio, T. Karapiperis, P. Kjaersgaard-Andersen, *Clin. Orthop. Relat. Res.* 478 (2020) 928–930.
- [10] L.M. Jennings, M. Al-Hajjar, C.L. Brockett, S. Williams, J.L. Tipper, E. Ingham, J. Fisher, *Orthop. Trauma* 26 (2012) 246–252.
- [11] C. Zietz, C. Fabry, J. Reinders, R. Dammer, J.P. Kretzer, R. Bader, R. Sonntag, *Expert Rev. Med. Devices* 12 (2015) 393–410.
- [12] A. Fischer, C. Beckmann, S. Heermant, A. Wittrock, P. Telouk, J. Debus, M.A. Wimmer, *Wear* 522 (2023) 204716.
- [13] F.P. Bowden, A.J.W. Moore, D. Tabor, 80 (1942).
- [14] C. Brown, S. Williams, J.L. Tipper, J. Fisher, E. Ingham, *J. Mater. Sci. Mater. Med.* 18 (2007) 819–827.
- [15] M.A. Wimmer, A. Fischer, R. Büscher, R. Pourzal, C. Sprecher, R. Hauert, J.J. Jacobs, *J. Orthop. Res.* (2009) n/a-n/a.
- [16] A. Fischer, S. Weiß, M.A. Wimmer, *J. Mech. Behav. Biomed. Mater.* 9 (2012) 50–62.
- [17] A. Mace, J.L. Gilbert, *Tribol. Int.* 180 (2023) 108222.
- [18] H.A. McKellop, D. D’Lima, *J. Am. Acad. Orthop. Surg.* 16 (2008) S111–S119.
- [19] R.M. Trommer, M.M. Maru, W.L. Oliveira Filho, V.P.S. Nykanen, C.P. Gouvea, B.S. Archanjo, E.H. Martins Ferreira, R.F. Silva, C.A. Achete, *Biotribology* 4 (2015) 1–11.
- [20] L. Mattei, F. Di Puccio, E. Ciulli, *Tribol. Int.* 63 (2013) 66–77.
- [21] Z. Hua, P. Dou, H. Jia, F. Tang, X. Wang, X. Xiong, L. Gao, X. Huang, Z. Jin, *Front. Mech. Eng.* 5 (2019).
- [22] A. Mace, (2022).
- [23] A. Igual Muñoz, N. Espallargas, in: *Tribocorrosion Passiv. Met. Coatings*, Elsevier, 2011, pp. 118–152.
- [24] M.T. Mathew, M.A. Wimmer, *Tribocorrosion in Artificial Joints: In Vitro Testing and Clinical Implications*, Woodhead Publishing Limited, 2013.
- [25] ASTM, (2020).
- [26] A. Mace, J.L. Gilbert, *Wear* 498–499 (2022) 204332.
- [27] J.D. Wernli, J.L. Gilbert, *J. Biomed. Mater. Res. Part A* 9999A (2009) NA-NA.
- [28] A. Hodgson, S. Kurz, S. Celene Virtanen, V. Fervel, C. Olsson, *Electrochim. Acta* (2004).
- [29] D. Landolt, S. Mischler, M. Stemp, *Electrochim. Acta* 46 (2001) 3913–3929.
- [30] R. He, S. Gahlawat, C. Guo, S. Chen, T. Dahal, H. Zhang, W. Liu, Q. Zhang, E. Chere, K. White, Z. Ren, *Phys. Status Solidi* 212 (2015) 2191–2195.
- [31] T.A. Simoes, M.G. Bryant, A.P. Brown, S.J. Milne, M. Ryan, A. Neville, R. Brydson, *Acta Biomater.* 45 (2016) 410–418.

- [32] S. Affatato, B. Fernandes, A. Tucci, L. Esposito, A. Toni, *Biomaterials* 22 (2001) 2325–2331.
- [33] M. Nine, D. Choudhury, A. Hee, R. Mootanah, N. Osman, *Materials (Basel)*. 7 (2014) 980–1016.
- [34] B. Thornley, R. Beadling, M. Bryant, A. Neville, *Corrosion* 76 (2020) 539–552.
- [35] I. Papageorgiou, Z. Yin, D. Ladon, D. Baird, A.C. Lewis, A. Sood, R. Newson, I.D. Learmonth, C.P. Case, *Mutat. Res. Mol. Mech. Mutagen.* 619 (2007) 45–58.
- [36] Y.-M. Kwon, Z. Xia, S. Glyn-Jones, D. Beard, H.S. Gill, D.W. Murray, *Biomed. Mater.* 4 (2009) 025018.
- [37] H.S. Gill, G. Grammatopoulos, S. Adshead, E. Tsiologiannis, E. Tsiroidis, *Trends Mol. Med.* 18 (2012) 145–155.
- [38] M.A. Koronfel, A.E. Goode, J.N. Weker, S.E.R. Tay, C.A. Stitt, T.A. Simoes, J.F.W. Mosselmanns, P. Quinn, R. Brydson, A. Hart, M.F. Toney, A.E. Porter, M.P. Ryan, *Npj Mater. Degrad.* 2 (2018) 1–5.
- [39] M.A. Koronfel, A.E. Goode, M.A. Gomez-Gonzalez, J.N. Weker, T.A. Simoes, R. Brydson, P. Quinn, M.F. Toney, A. Hart, A.E. Porter, M.P. Ryan, *J. Phys. Chem. C* 123 (2019) 9894–9901.
- [40] Y. Kim, J. Lim, *Sci. Rep.* 12 (2022) 1–8.
- [41] P.M. V Raja, A.R. Barron, *Nature* 134 (1934) 366–367.